



Molecular mechanism of the *miR-7/BCL2L1/P53* signaling axis regulating the progression of hepatocellular carcinoma

Nannan Zhang^{1,2#}, Feiran Wang^{2#}, Lirong Zhu^{2#}, Renan Chang², Shaffer R. S. Mok³, Renata D'Alpino Peixoto⁴, Weidong Tang², Zhong Chen^{1,2}

¹Medical College of Nantong University, Nantong, China; ²Department of General Surgery, Affiliated Hospital of Nantong University, Nantong, China; ³Department of Gastrointestinal Oncology, Moffitt Cancer Center, Tampa, FL, USA; ⁴Centro Paulista de Oncologia (Grupo Oncoclínicas), São Paulo, Brazil

Contributions: (I) Conception and design: N Zhang, F Wang; (II) Administrative support: L Zhu; (III) Provision of study materials or patients: R Chang; (IV) Collection and assembly of data: W Tang; (V) Data analysis and interpretation: Z Chen; (VI) Manuscript writing: All authors; (VII) Final approval of manuscript: All authors.

[#]These authors contributed equally to this work.

Correspondence to: Professor Zhong Chen. Medical College of Nantong University, Nantong 226000, China. Email: chenzgs@163.com.

Background: To investigate the roles of *miR-7* and its potential mechanisms in hepatocellular carcinoma (HCC).

Methods: The functions of *miR-7* were identified and measured by MTT [3-(4,5)-dimethylthiazolium(-z)-y1)-3,5-di-phenyltetrazolium bromide], colony formation, transwell, and flow cytometry assays. A luciferase assay was applied to verify the direct binding of *miR-7* on *BCL2L1* 3'untranslated region (3'UTR). An *in vitro* experiment was then used to investigate the biological effects of *miR-7* and *BCL2L1*. A co-immunoprecipitation (COIP) assay was used to detect the protein interaction between *BCL2L1* and *P53*.

Results: We found that *miR-7* overexpression suppressed cell proliferation, migration, and invasion in HCC. *BCL2L1* was also demonstrated as a direct target gene of *miR-7*. This study showed that *BCL2L1* could partially rescue the inhibitory effect of *miR-7* on the proliferation, migration, and invasion of HCC cells. Our research showed that *miR-7* could inhibit the epithelial-mesenchymal transition (EMT) pathway by regulating *BCL2L1*. We also further confirmed that *miR-7* inhibits the proliferation, migration, and invasion of Hep3B and Huh7 cells by targeting *BCL2L1*. Furthermore, we observed that the *BCL2L1* protein interacts with the *P53* protein and *BCL2L1* affects the development of liver cancer through *P53*. We also found that *BCL2L1* could promote the invasion and migration of liver cancer cells through *P53* inhibition. *BCL2L1* also inhibited the expression of Caspase 3/7 in hepatoma cells by inhibiting the expression of *P53*.

Conclusions: Our study demonstrated that *miR-7/BCL2L1/P53* may serve as a regulatory molecular axis for HCC treatment. Our results suggest that *miR-7/BCL2L1/P53* may have predictive value and represent a new treatment strategy for liver cancer.

Keywords: *miR-7*; hepatocellular carcinoma (HCC); *BCL2L1*; *P53*; metastasis

Submitted Oct 17, 2022. Accepted for publication Dec 23, 2022. Published online Jan 10, 2023.

doi: 10.21037/atm-22-5929

View this article at: <https://dx.doi.org/10.21037/atm-22-5929>

Introduction

Hepatocellular carcinoma (HCC) is the most common primary liver malignant tumor and the third leading cause of cancer-related death (1). At present, surgical resection and liver transplantation are the most effective treatment

methods, but the 5-year survival rate of liver cancer patients is still very low (2-4). Therefore, there is a pressing need to clarify the potential molecular mechanism of HCC and identify new possible targets to prevent the occurrence and development of this neoplasia.

In recent years, miRNA has become a hotspot in the field of tumor research, with numerous studies exploring *miRNAs*, providing new ideas for a more comprehensive and in-depth understanding of the pathogenesis of tumors (5). MiRNAs can act as either oncogenes or tumor suppressors and extensively participate in the emergence and development of various tumors (including liver cancer), through cell proliferation, apoptosis, and metastasis (6-8). Increasing evidence shows that abnormal miRNA expression participates in cancer occurrence by promoting the expression of proto-oncogenes or inhibiting the expression of tumor suppressor genes (9).

MiR-7 is involved in many signal pathways involved in differentiation, proliferation regulation, apoptosis and migration. It targets many mRNAs according to the intracellular environment, and is also regulated by different transcription factors and molecules involved in their processing and degradation (10). The study found that the level of miR-7 was related to the invasiveness of estrogen receptor positive breast tumors (11). Duex *et al.* found that *miR-7* forms a signaling pathway with epidermal growth factor receptor (*EGFR*) via Usp18 (Ubp43). Usp18 is a ubiquitin-specific peptidase, and its down-regulation can increase *miR-7* levels (12). It has been also found that miR-7 mediates hepatocyte growth factor (HGF) to inhibit the

activity of oncoprotein and inhibit the development of normal cells to cancer cells (13).

At present, there are few reports on the regulatory mechanism of *miR-7* in liver cancer and the specific functions and molecular mechanisms in hepatocarcinogenesis and development. Therefore, using *miR-7* as the research object, this study detected the expression of *miR-7* in liver cancer and further explored the specific functions and molecular mechanisms of *miR-7* in the process of hepatocarcinogenesis. We present the following article in accordance with the MDAR reporting checklist (available at <https://atm.amegroups.com/article/view/10.21037/atm-22-5929/rc>).

Methods

The RNA extraction and one-step reverse transcription quantitative real-time PCR (qRT-PCR) kits were purchased from Dayroot Biochemical Technology (Beijing, China); the Dulbecco's Modified Eagle Medium (DMEM) culture medium and fetal bovine serum (FBS) were purchased from the Gibco Company (New York, USA); the matrix glue was purchased from the Becton Dickinson (BD) Company (New York, USA); the Transwell Lab was purchased from the Corning Company (USA); and the β -Actin, *E-cadherin*, *N-cadherin*, *MMP2*, *MMP9*, *BCL2L1*, *P53*, *BAX*, *Caspase 3*, and *Caspase 7* antibodies were purchased from Proteintech (Chicago, USA).

Highlight box

Key findings

- This study found that BCL2L1 is a direct target gene of miR-7. BCL2L1 can partially rescue the inhibitory effect of miR-7 on the proliferation, migration and invasion of HCC cells. MiR-7 can inhibit the epithelial mesenchymal transformation (EMT) pathway by regulating BCL2L1. In addition, we found that BCL2L1 protein interacted with P53 protein. BCL2L1 also inhibits the expression of Caspase 3/7 in hepatoma cells by inhibiting the expression of P53.

What is known and what is new?

- MiR-7 mainly acts as a tumor suppressor and regulates some basic cellular processes, including proliferation, differentiation, apoptosis, and migration.
- Our study demonstrated that the *miR-7/BCL2L1/P53* signaling axis plays an important role in inhibiting the progression of liver cancer.

What is the implication, and what should change now?

- The *miR-7/BCL2L1/P53* may serve as a regulatory molecular axis for HCC treatment. These findings may provide a new therapeutic target for liver cancer.

Cell culture and transfection

The study conformed to the provisions of the Declaration of Helsinki (as revised in 2013), and was approved by the Ethics Committee of Affiliated Hospital of Nantong University (No. 2022-L094). Informed consent was provided by all participants. Fresh tissue and matched adjacent normal tissue samples from liver cancer patients were surgically removed at the Affiliated Hospital of Nantong University. None of the liver cancer patients received preoperative anti-tumor therapy. The *in vitro* culture human HCC cell lines (HCCLM3, Huh7, Hep3B) and human normal liver cell line (LO2) were purchased from ATCC (American type culture collection, Manassas, USA).

The cells were cultured in a 37 °C and 5% carbon dioxide (CO₂) environment. The overexpression plasmid, shRNA (short hairpin RNA), and negative control (NC) (Genechem, Shanghai, China) were transfected into cells with Lipofectamine 3000 reagent (Invitrogen, Carlsbad,

USA), and the transfection efficiency was evaluated with fluorescent qRT-PCR. The DMEM medium with 10% FBS concentration was used for the cell culture.

qRT-PCR

We used Trizol reagent (Invitrogen) to extract total RNA from cells and used a spectrophotometer to determine the purity and concentration of RNA according to the manufacturer's instructions. Total RNA (1 µg) was reverse transcribed into cDNA (complementary DNA) using the Prime Script RT kit (Takara Bio, Beijing, China). Using DNA as the template, the SYBR Select Master Mix kit (Thermo Fisher Scientific, Carlsbad, USA) and ABI Prism 7900 detection system (Applied Biosystems, Carlsbad, USA) were used for the qRT-PCR reaction. The primer sequences are listed as follows: *miR-7*, 5'-CGGGCCAACAAATCACAGTC-3' (forward) and 5'-CAGCCACAAAAGAGCACAAT-3' (reverse); and *BCL2L1*, 5'-CCTGACATCCCAGCTCCACA-3' (forward) and 5'-GCGATCCGACTCACCAATACC-3' (reverse).

Cell proliferation assay

Cell proliferation ability was analyzed using the MTT [3-(4,5)-dimethylthiazoliazol(2-yl)-2,5-diphenyltetrazolium bromide] test. Cells growing in the logarithmic phase were digested, counted, and then planted in a 96-well plate according to the appropriate density. MTT solution (200 µL) was added into each hole. Dimethyl sulfoxide (DMSO) (100 µL) was added into each hole after continuous cultivation for 4 h, and the culture plate was placed into the microplate reader (Olympus, Japan). We then detected the absorbance value of the optical density (OD)-490 nm holes (each group had three sets of auxiliary holes).

In addition, we also analyzed the proliferation ability of cells through colony formation assay. Cells were plated in 6-well plate at a density of 1,000 cells/plate. Two weeks later, the colony was fixed with 4% paraformaldehyde for 30 minutes, and stained with crystal violet for 10 minutes. All colonies were washed several times with ddH₂O, dried and photographed.

Cell apoptosis assay

Cell apoptosis was analyzed by flow cytometry. The cells were inoculated in the culture plate and transfected

after culturing for 24 h. The cells were collected 48 h after transfection, washed with phosphate buffer saline (PBS), and double stained using an Annexin V-FITC/PI (fluorescein isothiocyanate/propidium iodide) apoptosis detection kit (Solarbio, Beijing, China).

Cell migration assay

The cell migration ability was investigated using the cell scratch test. The cells were inoculated into six-well plates, cultured for 24 h, and then transfected. We used 10 µL sterile tips to scratch a single layer of cells, and the cells are washed with PBS three times to wash away the scratched cells. Serum-free DMEM was added and placed in the cell incubator for 24 hours. The scratches at 0 h and 72 h were photographed with an optical microscope (OLYMPUS, Tokyo, Japan) to calculate the cell migration rate. Finally, we took pictures.

Cell invasion experiment

A Transwell chamber (Thermo Fisher Scientific, Carlsbad, USA) was used to study the cell invasion ability. The transfected cells were digested and resuspended with serum-free DMEM medium, then added to the Transwell upper chamber coated with matrix glue, and the DMEM medium containing 10% FBS was added to the lower chamber. After placing the cells in the cell incubator for 24 h, cells on the membrane were gently removed, while cells under the membrane were fixed with methanol, stained with crystal violet, counted and took pictures.

Western blot analysis

Protein lysate was added to the cell culture plates of the experimental and control groups by western blot. The supernatant was centrifuged after ice lysis to determine the protein concentration of the two groups. Subsequently, the polyacrylamide gel was configured and equal proportions of protein samples of the control and experimental groups were placed into the upper sample well. We then performed constant flow electrophoresis until the protein lanes were fully separated.

The protein was transferred to a polyvinylidene fluoride (PVDF) membrane using the wet transfer method. After sealing using skimmed milk powder for 2 hours, we placed the cut PVDF membrane into the antibody incubation box and incubated it overnight at 4 °C. The next day, after TBS

with Tween-20 (TBST) rinsing, an HRP-labeled secondary antibody was added and incubated at room temperature for 1 h. A fully automated chemiluminescence imaging system (Odyssey, Ithaca, USA) was used to take photos.

Luciferase reporter assay

A target prediction and luciferase reporter gene experiment were carried out using the TARGETSCAN database (<https://www.targetscan.org/>) to predict the target gene of *hsa-miR-7*. Wild type (wt) and mutant type (mut) luciferase reporter gene plasmids were constructed. The luciferase reporter gene plasmid and miRNA overexpression plasmid were co-transfected into Huh7 cells, and the luciferase activity was determined using the double luciferase reporter gene system (Promega, Madison, USA).

Immunohistochemical staining

The paraffin-embedded sections were dewaxed and hydrated by immunohistochemical staining, and then washed twice using PBS for 5 min each time. Thereafter, 3% H₂O₂ (hydrogen peroxide) was sealed at room temperature for 5–10 min and then washed three times with distilled water for 5 min each time. Antigen repair was subsequently performed, PBS was used for washing (for 5 min), and bovine serum albumin (BSA) was used for sealing at room temperature (for 20 min). The first antibody was added dropwise and incubated overnight at 4 °C, and then washed with PBS three times (2 min each time). Next, a biotinylated secondary antibody was added dropwise for 20 min at 20–37 °C, and then washed with PBS three times (2 min each time). Subsequently, Strept Avidin-Biotin Complex (SABC) reagent was added dropwise for 20 min at 20–37 °C, washed with PBS four times (for 5 min each time), and then used the DAB (3,3'-diaminobenzidine) color development kit (Beyotime, Shanghai, China). We then washed this with distilled water three times (5 min each time), and subsequently used hematoxylin for 2 min and differentiated with hydrochloric acid ethanol. Thereafter, we performed dehydration, transparency, sealing film, and microscopic examination.

Statistical analysis

All data were analyzed using SPSS 26.0 software. The measurement data were expressed by ($\bar{x} \pm s$). Analysis of variance and the LSD-*t*-test were used to analyze the

differences between three groups, and the independent sample two-sided *f*-test was used to analyze the differences between two groups. $P < 0.05$ was considered to indicate a statistically significant difference.

Results

Overexpression of *miR-7* inhibits cell proliferation and metastasis

First, we detected the expression level of *miR-7* in HCC tissues and found that *miR-7* was lowly expressed (*Figure 1A*). To determine the possible mechanism of *miR-7* in HCC, we transfected a *miR-7* overexpression plasmid into Hep3B and Huh7 cells and also detected *miR-7* expression by qRT-PCR, which indicated that *miR-7* expression was significantly up-regulated (*Figure 1B*).

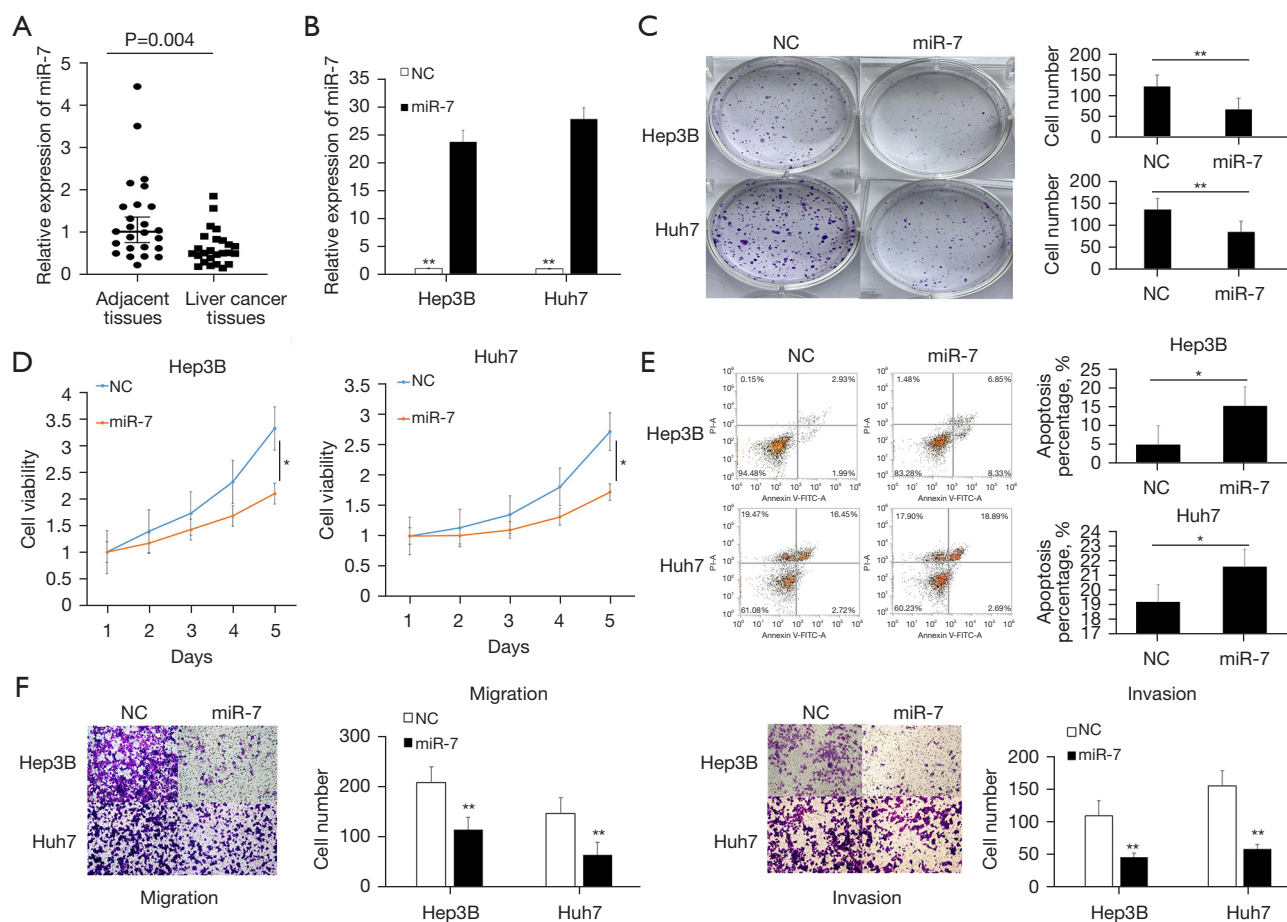
To further explore the function of *miR-7* in liver cancer cells, we used colony formation, MTT analysis, and flow cytometry analysis. Our colony formation and MTT analysis results showed that the proliferation and cell survival rates of the *miR-7* overexpression group were significantly reduced (*Figure 1C,1D*). In addition, flow cytometry analysis showed that *miR-7* overexpression markedly increased the number of apoptotic cells (*Figure 1E*). Moreover, Transwell analysis showed notably reduced migration and invasion in cells induced by *miR-7* (*Figure 1F*).

BCL2L1* is the target gene of *miR-7

The TARGETSCAN database (<https://www.targetscan.org/>) was utilized to predict the target gene of *hsa-miR-7*; we found that *BCL2L1* may be the target gene of *miR-7* (*Figure 2A*). The dual luciferase reporter gene experiment results showed that *miR-7* could significantly reduce the activity of the wt luciferase plasmid compared with the NC group (*Figure 2B*). At the same time, we overexpressed *miR-7* in Hep3B and Huh7 cells. The qPCR results showed that overexpression of *miR-7* could substantially inhibit the expression of *BCL2L1* (*Figure 2C*).

The high expression of *BCL2L1* in liver cancer tissues and cells was determined via The Cancer Genome Atlas (TCGA) and Gene Expression Profiling Interactive Analysis (GEPIA) databases

To investigate the expression of *BCL2L1* in different tumors, we conducted differential expression analysis using TCGA



(<https://cancergenome.nih.gov/>) and GEPIA databases [Gene Expression Profiling Interactive Analysis (GEPIA), cancer-pku.cn]. Our results showed that, compared with normal tissues, *BCL2L1* was notably overexpressed in tumors such as uterine corpus endometrial carcinoma, breast cancer, cervical squamous cell carcinoma and endocervical adenocarcinoma, prostate adenocarcinoma, HCC, etc. (Figure 3A). Subsequently, we further analyzed the expression level of *BCL2L1* in liver cancer tissue. The results showed that *BCL2L1* was significantly overexpressed in liver cancer compared with the adjacent tissues (Figure 3B). Paired difference analysis further confirmed that

BCL2L1 was highly expressed in HCC (Figure 3C).

To further explore the biological function of *BCL2L1*, we carried out co-expression and function enrichment analyses of the *BCL2L1* gene. Figure 3D shows 21 co-expressed genes that are correlated with *BCL2L1*. Subsequently, we selected the first 100 co-expressed genes with the highest correlation for enrichment analysis (Figure 3E), in which the neuroactive ligand-receptor interaction was the highly enriched Gene Ontology (GO) terms (Figure 3F). In addition, we also performed a logistic analysis of the correlation between *BCL2L1* expression and clinicopathological features using TCGA database. We found that the high expression

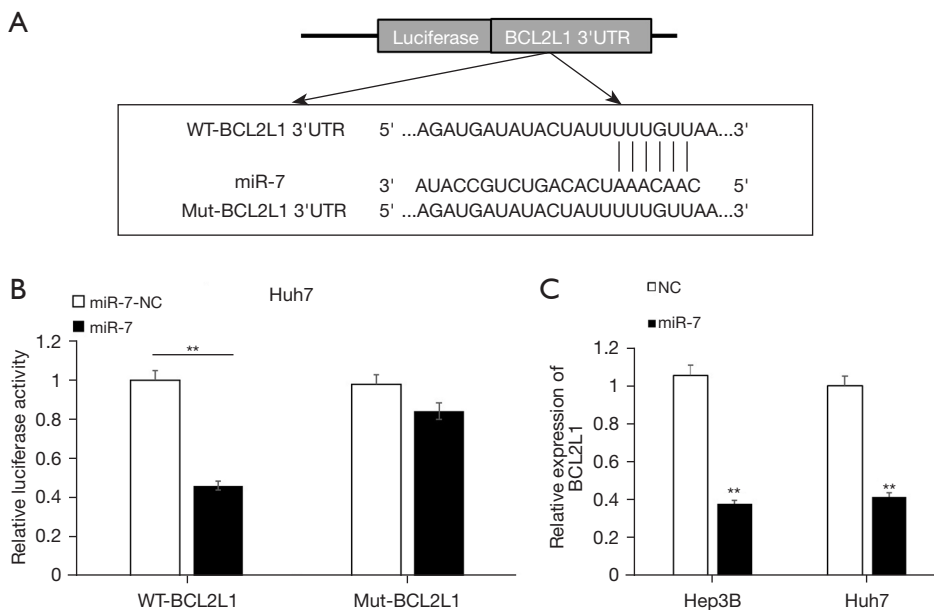


Figure 2 *BCL2L1* was predicted to be the target of *miR-7*. (A) The sequences of *miR-7* binding sites within the *BCL2L1* 3'UTR and schematic reporter constructs. *BCL2L1* WT represents the reporter constructs containing the 3'UTR sequences of *BCL2L1*. *BCL2L1* MUT represents the reporter constructs containing mutated nucleotides. (B) Luciferase reporter assay of Huh7 cells co-transfected with pGL3-*BCL2L1*-3'UTR-WT or pGL3-*BCL2L1*-3'UTR-Mut reporter and miR-NC or *miR-7*. The relative luciferase activity was detected after transfection. (C) qRT-PCR analysis of the expression level of *BCL2L1* in Hep3B and Huh7 cells. **, $P < 0.01$. WT, wild type; UTR, untranslated region; NC, negative control; qRT-PCR, quantitative real-time PCR.

of *BCL2L1* was related to the T stage, pathologic stage, and HISTOLOGIC grade (Table 1).

The high expression of *BCL2L1* in liver cancer tissues was detected by western blot, qPCR, and immunohistochemistry

To verify the expression of *BCL2L1* in liver cancer tissues, we detected the *BCL2L1* protein expression in liver cancer and normal adjacent tissues by western blot. The results showed that the *BCL2L1* protein expression in liver cancer tissues was significantly higher than that in adjacent tissues, and the difference was statistically significant (Figure 4A). We also found that *BCL2L1* was highly expressed in HCC cells (Figure 4B).

Next, qRT-PCR was applied to detect the *BCL2L1* mRNA expression in 25 pairs of liver cancer and adjacent normal tissues, which was significantly higher than that in the corresponding adjacent liver tissues (Figure 4C), and the expression of *BCL2L1* in HCC was negatively correlated with the expression of *miR-7* (Figure 4D).

Immunohistochemistry showed that the *BCL2L1* protein expression in liver cancer and adjacent tissues

showed brown-yellow diffuse staining, and its expression was mainly localized in the cytoplasm (Figure 4E). Among 121 liver cancer tissues, *BCL2L1* was expressed in 75 cases (61.9%), and was positive in 15 of 46 adjacent tissues, with a positive rate of 31.9%. The expression of *BCL2L1* in liver cancer tissues was markedly different from that in adjacent tissues ($P < 0.05$). In addition, we also found that the positive expression of *BCL2L1* in HCC was related to tumor size, tumor node metastasis (TNM) stage, and tumor size. However, there was no significant correlation with the gender, age, number of tumors, degree of differentiation, HBV infection, and degree of liver cirrhosis of liver cancer patients (Table 2).

Effect of silencing *BCL2L1* on the invasion, migration, and apoptosis of HCC cells

First, *sh-BCL2L1* (*BCL2L1* interference plasmid) was used to silence the expression of *BCL2L1* in Hep3B and Huh7 cells, and the interference effect was detected by western blot (Figure 5A). The flow cytometry results showed that *sh-BCL2L1* could significantly inhibit the apoptosis of Hep3B

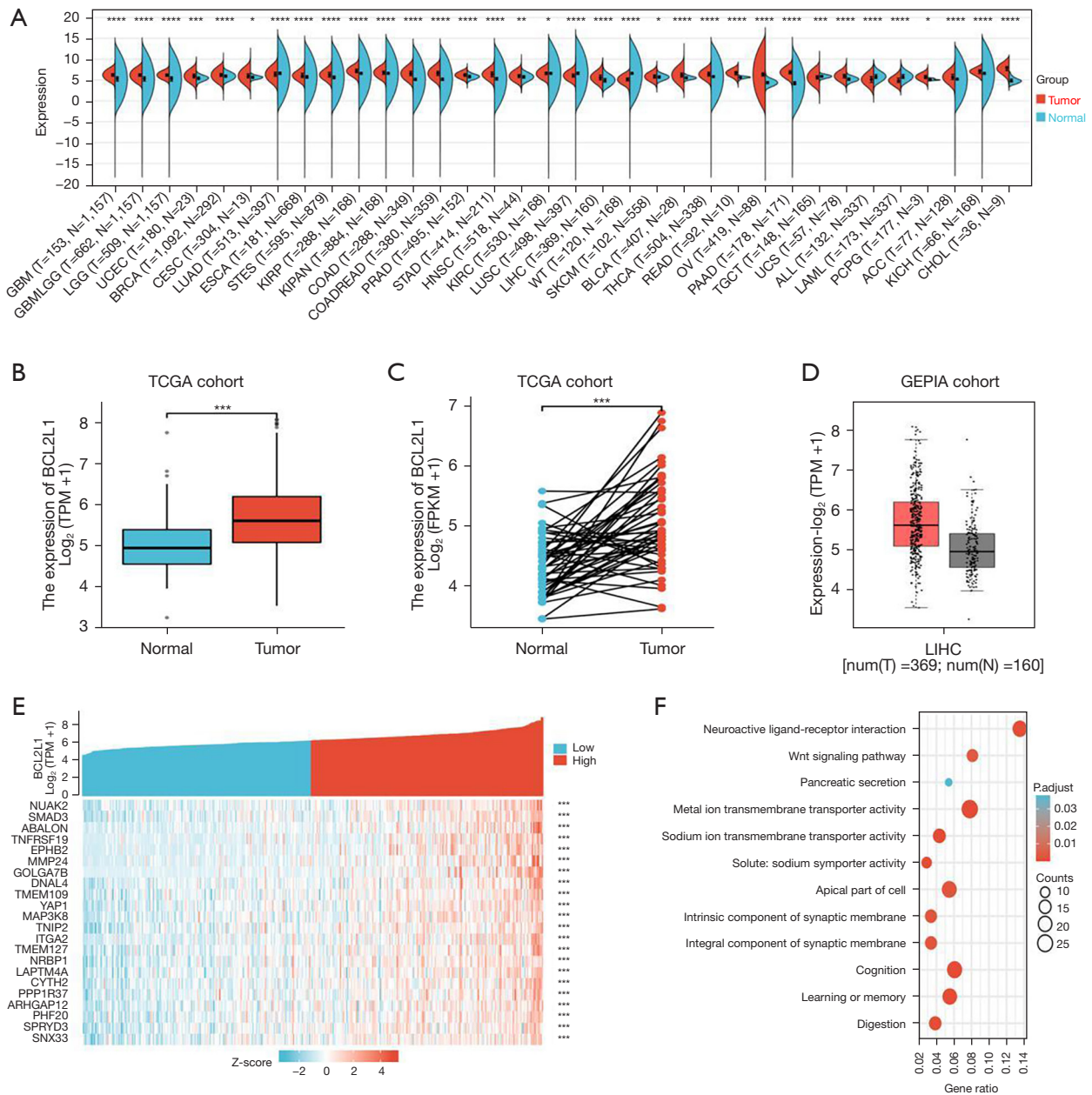


Figure 3 The high expression of *BCL2L1* in HCC was confirmed through the TCGA-LIHC and GEPIA datasets. (A) *BCL2L1* was significantly overexpressed in tumors such as UCEC, BREAST, CESC, PRAD, LIHC, etc., compared with normal tissues from the TCGA-LIHC dataset. (B) *BCL2L1* was significantly overexpressed in liver cancer compared with adjacent tissues from the TCGA-LIHC dataset. (C) Paired difference analysis further confirmed that *BCL2L1* was highly expressed in HCC from the TCGA-LIHC dataset. (D) *BCL2L1* was significantly overexpressed in liver cancer compared with adjacent tissues from the GEPIA dataset. (E) Twenty-one co-expressed genes were correlated with *BCL2L1*. (F) The first 100 co-expressed genes with the highest correlation for enrichment analysis. *, P<0.05; **, P<0.01; ***, P<0.001; ****, P<0.0001. TCGA, The Cancer Genome Atlas; GEPIA, Gene Expression Profiling Interactive Analysis; TPM, transcript per million; HCC, hepatocellular carcinoma; LIHC, liver hepatocellular carcinoma.

Table 1 Logistic analysis of the correlation between *BCL2L1* expression and clinicopathological features

Characteristics	Total (N)	OR	P value
T stage (T3 & T4 vs. T1 & T2)	371	1.723 (1.073–2.793)	0.025*
N stage (N1 vs. N0)	258	2.603 (0.328–53.007)	0.410
M stage (M1 vs. M0)	272	2.662 (0.336–54.188)	0.399
Pathologic stage (stages III & IV vs. stages I & II)	350	2.045 (1.257–3.365)	0.004*
Tumor status (with tumor vs. tumor-free)	355	1.218 (0.800–1.857)	0.359
Gender (male vs. female)	374	0.885 (0.573–1.365)	0.581
BMI (kg/m ²) (>25 vs. ≤25)	337	0.775 (0.504–1.189)	0.244
Residual tumor (R1 & R2 vs. R0)	345	2.113 (0.800–6.194)	0.144
Histologic grade (G3 & G4 vs. G1 & G2)	369	1.639 (1.072–2.519)	0.023*
Adjacent hepatic tissue inflammation (mild & severe vs. none)	237	1.532 (0.918–2.567)	0.103
AFP (ng/mL) (>400 vs. ≤400)	280	1.482 (0.850–2.603)	0.167
Albumin (g/dL) (≥3.5 vs. <3.5)	300	1.194 (0.697–2.059)	0.519
Prothrombin time (>4 vs. ≤4)	297	1.331 (0.810–2.195)	0.260
Child-Pugh grade (B & C vs. A)	241	2.327 (0.942–6.299)	0.077
Fibrosis Ishak score (3/4 & 5/6 vs. 0 & 1/2)	215	0.945 (0.553–1.615)	0.837
Vascular invasion (yes vs. no)	318	0.983 (0.619–1.561)	0.942

*, P<0.05. OR, odds ratio; BMI, body mass index; AFP, alpha fetoprotein.

and Huh7 cells compared with the NC group (*Figure 5B*). The wound healing (*Figure 5C*) and Transwell test (*Figure 5D*) results showed that *sb-BCL2L1* could considerably inhibit the migration and invasion of Hep3B and Huh7 cells compared with the NC group.

The BCL2L1 mechanism promotes the invasion and migration of liver cancer cells and inhibits apoptosis of liver cancer cells

The STRING database [functional protein association networks (STRING), string-db.org] was used to predict and validate the *BCL2L1*-interacting proteins. We found that the *P53* and *BAX* proteins may be *BCL2L1*-interacting proteins (*Figure 6A*). The co-immunoprecipitation (COIP) experiment results also showed that the *BCL2L1* protein interacted with the *P53* and *BAX* proteins. At the same time, we silenced the expression of *BCL2L1* in Hep3B and Huh7 cells, and through western blot, observed that the expression of *P53* was reduced. Moreover, *sb-BCL2L1* could significantly inhibit the expressions of *P53* and *BAX* (*Figure 6B*). Western blot also demonstrated that E-cadherin was

up-regulated in Hep3B and Huh7 cells, while N-cadherin, MMP2, and MMP9 were down-regulated (*Figure 6C*). Therefore, *BCL2L1* may promote the invasion and migration of liver cancer cells through the epithelial-mesenchymal transition (EMT) pathway.

Regulatory mechanism of the miR-7/BCL2L1 signaling axis in HCC

To determine whether *miR-7* inhibition of Huh7 cell invasion and migration is the result of *miR-7* targeting *BCL2L1*, we restored the expression of *BCL2L1* inhibited by *miR-7* through a recovery experiment. Our results indicated that the restoration of *BCL2L1* expression in Hep3B and Huh7 cells eliminated the *miR-7* inhibition of cell invasion and migration (*Figure 7A, 7B*). The Western Blot results also showed that overexpression of *miR-7* could substantially inhibit the expression of *BCL2L1*. To further confirm whether *miR-7* is related to the EMT pathway via *BCL2L1* regulation, we transfected HCC cells with *miR-7* and *BCL2L1* overexpression plasmids. The *miR-7* overexpression plasmid up-regulated the expression

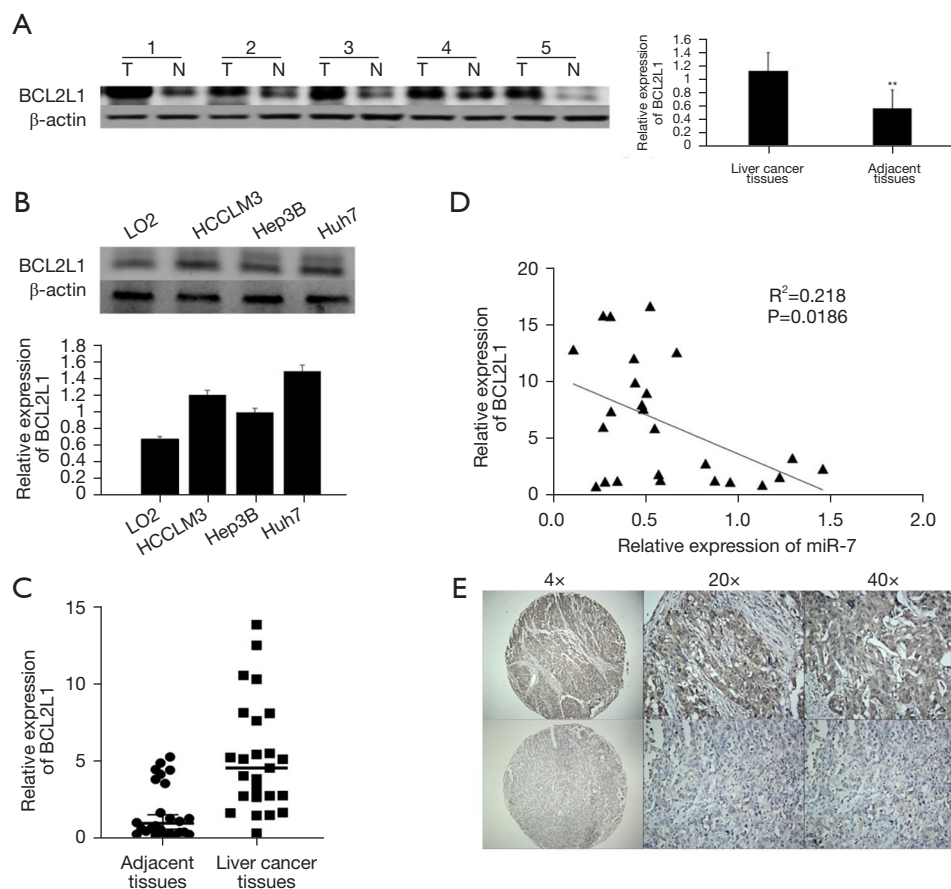


Figure 4 High expression of *BCL2L1* in liver cancer tissues and cells. (A) *BCL2L1* protein expression in liver cancer tissues was found to be significantly higher than that in adjacent tissues by western blot analysis, and the difference was statistically significant. (B) *BCL2L1* was highly expressed in HCC cells. (C) The expression of *BCL2L1* mRNA in 25 pairs of liver cancer and adjacent normal tissues by qRT-PCR. The results showed that the *BCL2L1* mRNA expression level in liver cancer tissues was significantly higher than that in the corresponding adjacent liver tissues. (D) The expression of *BCL2L1* in HCC was negatively correlated with the miR-7 expression. (E) Immunohistochemistry (took pictures under the $\times 4$, $\times 20$ and $\times 40$ mirrors respectively) showed that the expression of the *BCL2L1* protein in breast cancer tissues and adjacent tissues displayed brown-yellow diffuse staining, and its expression was mainly localized in the cytoplasm. **, $P < 0.01$. HCC, hepatocellular carcinoma; qRT-PCR, quantitative real-time PCR.

of E-cadherin, and down-regulated the expression of *N-cadherin*, *MMP2*, and *MMP9* in Hep3B and Huh7 cells. *BCL2L1* overexpression eliminates these effects. Our results consistently showed that *miR-7* hinders the progression of liver cancer by inhibiting *BCL2L1* (Figure 7C).

Regulatory mechanism of the *BCL2L1/P53* signaling axis in HCC

To clarify whether *BCL2L1* affects the invasion and migration of HCC and *Caspase 3/7* through *P53*, we transfected *sb-BCL2L1* and *P53* overexpression plasmids

into Hep3B and Huh7 cells. Compared with the control cells, the migration and invasion of *P53*-transfected Hep3B and Huh7 cells were significantly inhibited (Figure 8A). *BCL2L1* overexpression could partially rescue the promotion of *P53* silencing on *Caspase 3/7*. Furthermore, it could be seen that *BCL2L1* plays a role in the progression of liver cancer by regulating *P53* (Figure 8B).

Discussion

Although previous studies have shown that epigenetic and molecular changes of various well-known signaling

Table 2 Relationship between *BCL2L1* expression and clinicopathological parameters in liver tissue

Group	N	<i>BCL2L1</i> (n), high/low	χ^2	P value
Age			1.486	0.323
>50 years	87	51/36		
≤50 years	34	24/10		
Gender			0.062	0.803
Male	104	64/40		
Female	17	11/6		
Tumor size (cm)			4.139	0.042*
<5	59	42/17		
≥5	62	33/29		
Tumor number			0.536	0.464
Single	82	49/33		
Multiple	39	26/13		
TNM			3.917	0.048*
I/II	76	42/34		
III/IV	45	33/12		
Differentiation degree			0.035	0.851
Well/moderate	75	46/29		
Poor	46	29/17		
HBsAg			0.157	0.692
Negative	14	8/6		
Positive	107	67/40		
Cirrhosis			3.294	0.070
No	46	35/11		
Yes	75	45/30		

*, P<0.05. TNM, tumor node metastasis; HBsAg, hepatitis B surface antigen.

pathways are involved in the genesis and development of HCC, the molecular mechanism of HCC has not been fully elucidated (14). In recent years, molecular targeted therapy of liver cancer has become a research hotspot, and there is a pressing need to identify effective key therapeutic targets for liver cancer.

The expression of *miR-7* is usually down-regulated in different cancer cells [i.e., brain, lung, and colon cancer cells (15-18)]. In mammals, *miR-7* mainly acts as a tumor suppressor and regulates some basic cellular processes, including proliferation, differentiation, apoptosis, and migration (19,20). Interestingly, it is also involved in the

signaling pathway that guides the differentiation of different tissues and is regulated by specific transcription factors (21). For example, *miR-7* can inhibit cell metastasis by targeting focal adhesion kinase (FAK) and Kruppel-like factor 4 (KLF4) in breast cancer (22,23). *miR-7* inhibits proliferation and metastasis by regulating the *PI3K/Akt* signaling pathway in HCC and glioblastoma (24). In tumor stem cells, the *miR-7* promoter is silenced due to DNA methylation (25). In breast cancer, its expression depends on estrogen (26). It was found that *miR-7* is a new and reliable biomarker of an acidic tumor microenvironment (TME) and a novel therapeutic target for non-small cell lung cancer (NSCLC) (27). Ku

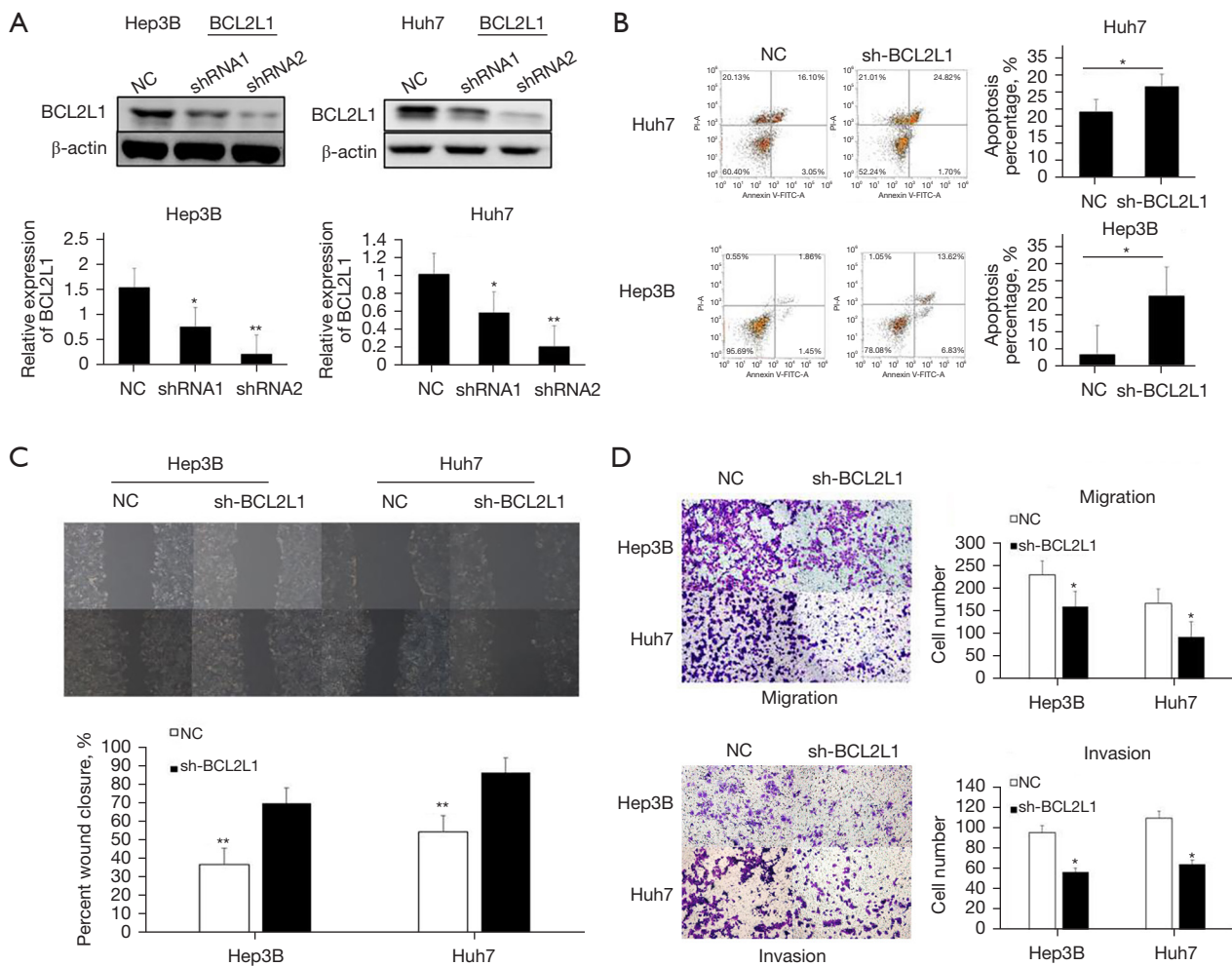


Figure 5 Knockout of *BCL2L1* inhibits the invasion and migration of HCC cells and promotes apoptosis. (A) The *BCL2L1* protein expression level in Hep3B and Huh7 cells was determined by western blot analysis. (B) Cell apoptosis was measured by flow cytometry assay after transfection of sh-*BCL2L1*. (C,D) Cell migration and invasion were analyzed using a transwell assay (stained with crystal violet, original magnification $\times 100$) and wound healing following transfection (original magnification $\times 100$) of sh-*BCL2L1*. *, $P < 0.05$; **, $P < 0.01$. NC, negative control; HCC hepatocellular carcinoma; FITC, fluorescein isothiocyanate; PI, propidium iodide.

et al. found that LINC00240 acts as a sponge for *miR-7-5p* and induces EGFR overexpression. Also, LINC00240 knockdown induces *miR-7-5p* overexpression (28). However, the mechanism of *miR-7* in HCC remains unclear.

The present study evaluated the expression and function of *miR-7* in HCC. The results showed that *miR-7* expression was down-regulated in HCC. *miR-7* inhibited the proliferation, migration, and invasion of Hep3B and Huh7 cells, and promoted the apoptosis of Hep3B and Huh7 cells. Moreover, to further evaluate the molecular mechanism of *miR-7* inhibiting hepatocarcinogenesis, we predicted that *BCL2L1* was the target gene of *miR-7* using the TargetScan

and StarBase software, and confirmed that *BCL2L1* was the target gene of *miR-7* through a dual luciferase experiment. It has been confirmed that the members of B-cell CLL/lymphoma 2 (*BCL-2*) family proteins play a central role in determining the occurrence of apoptosis by regulating the permeability of the mitochondrial outer membrane. *BCL2L1* counteracts its apoptosis-promoting function by preventing *BAX* and *BAD* transfer from the cytoplasm to mitochondria (29). Furthermore, it has also been reported that *miR-1266* and *miR-185* can induce cell apoptosis and reduce proliferation by inhibiting the *BCL2* and *BCL2L1* genes (30).

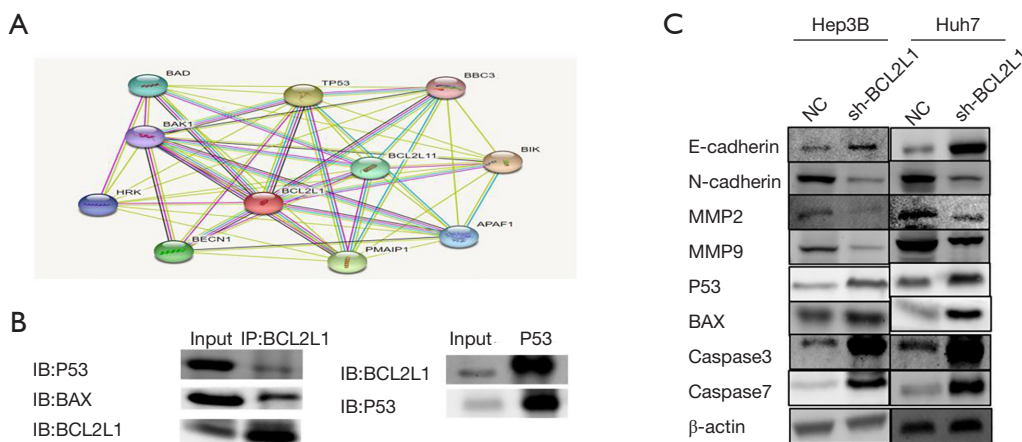


Figure 6 The P53 and BAX proteins are *BCL2L1*-interacting proteins and the *BCL2L1* promotes the invasion and migration of liver cancer cells through the EMT pathway. (A) Predictions of *BCL2L1*-interacting proteins were made using STRING software. (B) Protein interaction between *BCL2L1* and *P53/BAX*. (C) The expression of E-cadherin, N-cadherin, MMP2, MMP9, P53, BAX, and Caspase 3/7 at the protein level in transfected cells with sh-NC or sh-*BCL2L1* were examined by western blot analysis. IB, immunoblotting; IP, immunoprecipitation; NC, negative control; MMP, matrix metallopeptidase; EMT, epithelial-mesenchymal transition.

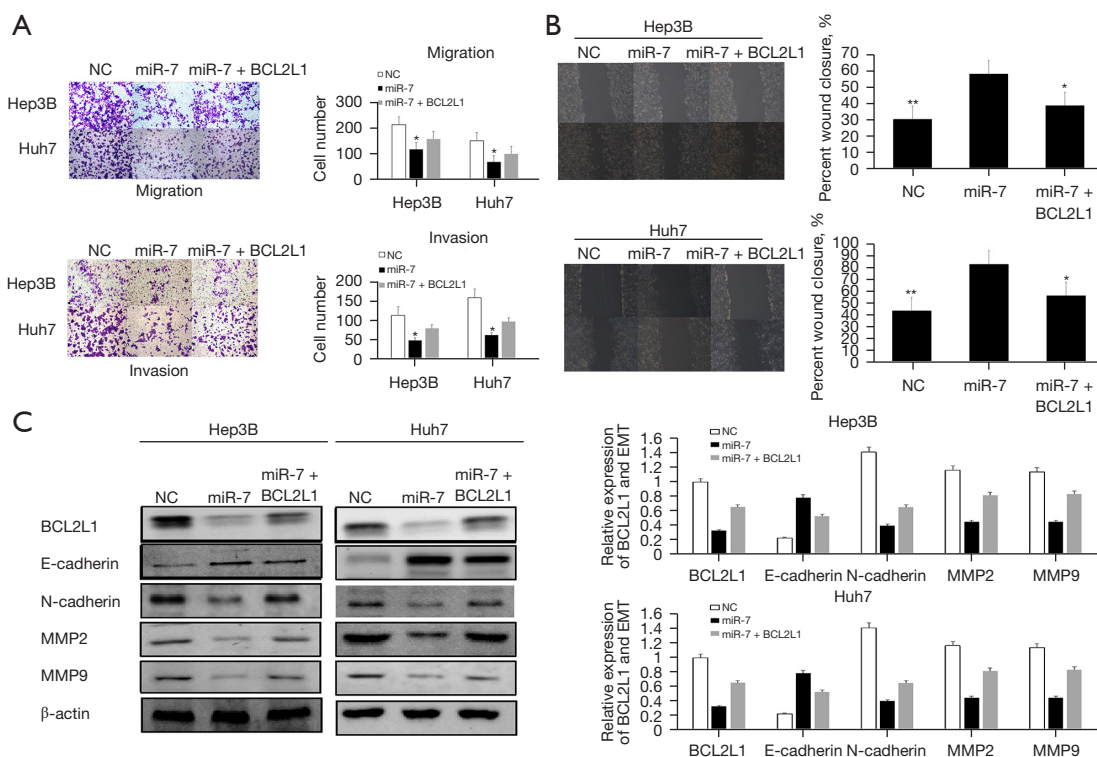


Figure 7 *BCL2L1* overexpression rescued the *miR-7*-mediated inhibitory effects in HCC cells. (A,B) The inhibitory functions of *miR-7* on cell migration and invasion were measured by Transwell assays (A) (stained with crystal violet, original magnification $\times 100$) and wound healing (B) (original magnification $\times 100$) in Hep3B and Huh7 cells transfected with the *BCL2L1* overexpression plasmid, respectively. (C) The expressions levels of E-cadherin, N-cadherin, MMP2, and MMP9 were detected by western blot analysis in Hep3B and Huh7 cells that were transfected with sh-NC, *miR-7*, or *miR-7 + BCL2L1*, respectively. *, $P < 0.05$; **, $P < 0.01$. NC, negative control; HCC, hepatocellular carcinoma; MMP, mitochondrial membrane potential.

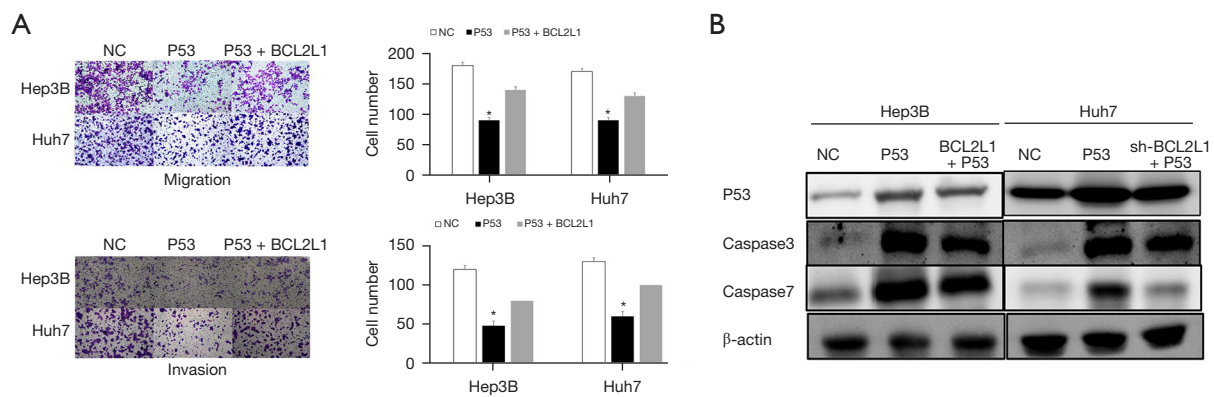


Figure 8 Regulatory mechanism of the *BCL2L1/P53* signaling axis in HCC. (A) The inhibitory functions of *P53* on cell migration and invasion were measured using a Transwell (stained with crystal violet, original magnification $\times 100$) in Hep3B and Huh7 cells transfected with the *BCL2L1* overexpression plasmid. (B) The expressions levels of Caspase 3/7 were detected by western blot analysis in Hep3B and Huh7 cells that were transfected with sh-NC, *P53*, or *P53 + BCL2L1*, respectively. *, $P < 0.05$. NC, negative control.

In addition, studies have demonstrated that *BCL2L1* also participates in cell migration and mitochondrial metabolism, in addition to its effect on apoptosis. These effects may be conducive to the occurrence and diffusion of transfer (31). Increased *BCL2L1* is related to the drug resistance of ovarian cancer to a variety of anti-cancer drugs. The double inhibition of *FGFR4* and *BCL2L1* has shown strong effects and tolerable toxicity (32). Thus, *BCL2L1* plays an important role in the occurrence and development of tumors. We found that *BCL2L1* is highly expressed in HCC. We also found that the positive expression of *BCL2L1* in HCC was related to tumor size, TNM stage and tumor size. In addition, silencing *BCL2L1* can significantly inhibit the proliferation, invasion and migration of HCC cells and promote apoptosis. Therefore, *BCL2L1* plays an important role in the occurrence and development of liver cancer.

The abnormal reactivation of EMT is related to the malignant characteristics of tumor cells during tumor progression and metastasis, such as promoting migration and invasion, increasing tumor stem cells, and enhancing resistance to chemotherapy and immunotherapy (33,34). The knockdown of *BCL2L1* expression increases the expression of *E-cadherin* in the EMT signaling pathway of liver cancer cells and decreases the expression of *N-cadherin*, *MMP2*, and *MMP9*. Thus, *BCL2L1* promotes the invasion and migration of liver cancer cells through the EMT signal pathway.

We also found that *BCL2L1* may inhibit the apoptosis of hepatoma cells through *P53*, *BAX*, and *Caspase 3/7*.

In this study, we used bioinformatics software to predict proteins and the COIP experiment to verify that *P53* and *BAX* are the *BCL2L1*-interacting proteins. We also found that *BCL2L1* can partially rescue the inhibitory effect of *miR-7* on the proliferation, migration, and invasion of HCC cells. Our research shows that *miR-7* can inhibit the EMT pathway by regulating *BCL2L1*. In addition, *BCL2L1* overexpression can partially rescue the inhibition of *P53* on the invasion and migration of HCC cells. *BCL2L1* overexpression can also partially rescue the promotion of *P53* silencing on *Caspase 3/7*. These results indicate that *BCL2L1* plays a role in the progression of liver cancer by regulating *P53*.

In conclusion, the *miR-7/BCL2L1/P53* signaling axis plays an important role in inhibiting the progression of liver cancer. These findings may provide an effective therapeutic target for liver cancer.

Conclusions

In summary, we demonstrated that *BCL2L1* is a direct target gene of *miR-7*. *miR-7* can inhibit the epithelial mesenchymal transformation (EMT) pathway by regulating *BCL2L1*. In addition, we found that *BCL2L1* protein interacted with *P53* protein. *BCL2L1* also inhibits the expression of *Caspase 3/7* in hepatoma cells by inhibiting the expression of *P53*. Consequently, further research is needed to clarify the regulation mechanism *miR-7/BCL2L1/P53* axis and identify specific targets for HCC treatment.

Acknowledgments

The authors appreciate the academic support from the AME Hepatocellular Carcinoma Collaborative Group.

Funding: This work was supported by grants from the Jiangsu Postgraduate Research and Practice Innovation Program (Grant No. KYCX21_3110 to Nannan Zhang), the National Science Fund for Distinguished Young Scholars (Grant No. 20925520), and the National Natural Science Foundation of China (Grant Nos. 21235003, 81172503).

Footnote

Reporting Checklist: The authors have completed the MDAR reporting checklist. Available at <https://atm.amegroups.com/article/view/10.21037/atm-22-5929/rc>

Data Sharing Statement: Available at <https://atm.amegroups.com/article/view/10.21037/atm-22-5929/dss>

Conflicts of Interest: All authors have completed the ICMJE uniform disclosure form (available at <https://atm.amegroups.com/article/view/10.21037/atm-22-5929/coif>). SRSM received Consulting fees from ConMed. The other authors have no conflicts of interest to declare.

Ethical Statement: The authors are accountable for all aspects of the work in ensuring that questions related to the accuracy or integrity of any part of the work are appropriately investigated and resolved. The study conformed to the provisions of the Declaration of Helsinki (as revised in 2013), and was approved by the Ethics Committee of Affiliated Hospital of Nantong University (No. 2022-L094). Informed consent was provided by all participants.

Open Access Statement: This is an Open Access article distributed in accordance with the Creative Commons Attribution-NonCommercial-NoDerivs 4.0 International License (CC BY-NC-ND 4.0), which permits the non-commercial replication and distribution of the article with the strict proviso that no changes or edits are made and the original work is properly cited (including links to both the formal publication through the relevant DOI and the license). See: <https://creativecommons.org/licenses/by-nc-nd/4.0/>.

References

1. Roberts LR. Sorafenib in liver cancer--just the beginning. *N Engl J Med* 2008;359:420-2.
2. Olsen SK, Brown RS, Siegel AB. Hepatocellular carcinoma: review of current treatment with a focus on targeted molecular therapies. *Therap Adv Gastroenterol* 2010;3:55-66.
3. Anwanwan D, Singh SK, Singh S, et al. Challenges in liver cancer and possible treatment approaches. *Biochim Biophys Acta Rev Cancer* 2020;1873:188314.
4. Sun JH, Luo Q, Liu LL, et al. Liver cancer stem cell markers: Progression and therapeutic implications. *World J Gastroenterol* 2016;22:3547-57.
5. Mishra S, Yadav T, Rani V. Exploring miRNA based approaches in cancer diagnostics and therapeutics. *Crit Rev Oncol Hematol* 2016;98:12-23.
6. Rupaimoole R, Slack FJ. MicroRNA therapeutics: towards a new era for the management of cancer and other diseases. *Nat Rev Drug Discov* 2017;16:203-22.
7. Zhou X, Zhang CZ, Lu SX, et al. miR-625 suppresses tumour migration and invasion by targeting IGF2BP1 in hepatocellular carcinoma. *Oncogene* 2016;35:5078.
8. Hou J, Lin L, Zhou W, et al. Identification of miRNomes in human liver and hepatocellular carcinoma reveals miR-199a/b-3p as therapeutic target for hepatocellular carcinoma. *Cancer Cell* 2011;19:232-43.
9. Iacona JR, Lutz CS. miR-146a-5p: Expression, regulation, and functions in cancer. *Wiley Interdiscip Rev RNA* 2019;10:e1533.
10. Korać P, Antica M, Matulić M. MiR-7 in Cancer Development. *Biomedicines* 2021;9:325.
11. Foekens JA, Sieuwerts AM, Smid M, et al. Four miRNAs associated with aggressiveness of lymph node-negative, estrogen receptor-positive human breast cancer. *Proc Natl Acad Sci U S A* 2008;105:13021-6.
12. Duex JE, Comeau L, Sorkin A, et al. Usp18 regulates epidermal growth factor (EGF) receptor expression and cancer cell survival via microRNA-7. *J Biol Chem* 2011;286:25377-86.
13. Jeong D, Ham J, Park S, et al. MicroRNA-7-5p mediates the signaling of hepatocyte growth factor to suppress oncogenes in the MCF-10A mammary epithelial cell. *Sci Rep* 2017;7:15425.
14. El-Serag HB, Rudolph KL. Hepatocellular carcinoma: epidemiology and molecular carcinogenesis.

- Gastroenterology 2007;132:2557-76.
15. Saydam O, Senol O, Würdinger T, et al. miRNA-7 attenuation in Schwannoma tumors stimulates growth by upregulating three oncogenic signaling pathways. *Cancer Res* 2011;71:852-61.
 16. Zhao J, Wang K, Liao Z, et al. Promoter mutation of tumor suppressor microRNA-7 is associated with poor prognosis of lung cancer. *Mol Clin Oncol* 2015;3:1329-36.
 17. Zhang N, Li X, Wu CW, et al. microRNA-7 is a novel inhibitor of YY1 contributing to colorectal tumorigenesis. *Oncogene* 2013;32:5078-88.
 18. Midgley AC, Morris G, Phillips AO, et al. 17 β -estradiol ameliorates age-associated loss of fibroblast function by attenuating IFN- γ /STAT1-dependent miR-7 upregulation. *Aging Cell* 2016;15:531-41.
 19. Pogribny IP, Filkowski JN, Tryndyak VP, et al. Alterations of microRNAs and their targets are associated with acquired resistance of MCF-7 breast cancer cells to cisplatin. *Int J Cancer* 2010;127:1785-94.
 20. Fang Y, Xue JL, Shen Q, et al. MicroRNA-7 inhibits tumor growth and metastasis by targeting the phosphoinositide 3-kinase/Akt pathway in hepatocellular carcinoma. *Hepatology* 2012;55:1852-62.
 21. Marzioni M, Agostinelli L, Candelaresi C, et al. Activation of the developmental pathway neurogenin-3/microRNA-7a regulates cholangiocyte proliferation in response to injury. *Hepatology* 2014;60:1324-35.
 22. Okuda H, Xing F, Pandey PR, et al. miR-7 suppresses brain metastasis of breast cancer stem-like cells by modulating KLF4. *Cancer Res* 2013;73:1434-44.
 23. Kong X, Li G, Yuan Y, et al. MicroRNA-7 inhibits epithelial-to-mesenchymal transition and metastasis of breast cancer cells via targeting FAK expression. *PLoS One* 2012;7:e41523.
 24. Kefas B, Godlewski J, Comeau L, et al. microRNA-7 inhibits the epidermal growth factor receptor and the Akt pathway and is down-regulated in glioblastoma. *Cancer Res* 2008;68:3566-72.
 25. Xin L, Liu L, Liu C, et al. DNA-methylation-mediated silencing of miR-7-5p promotes gastric cancer stem cell invasion via increasing Smo and Hes1. *J Cell Physiol* 2020;235:2643-54.
 26. Masuda M, Miki Y, Hata S, et al. An induction of microRNA, miR-7 through estrogen treatment in breast carcinoma. *J Transl Med* 2012;10 Suppl 1:S2.
 27. Su T, Huang S, Zhang Y, et al. miR-7/TGF- β 2 axis sustains acidic tumor microenvironment-induced lung cancer metastasis. *Acta Pharm Sin B* 2022;12:821-37.
 28. Ku GW, Kang Y, Yu SL, et al. LncRNA LINC00240 suppresses invasion and migration in non-small cell lung cancer by sponging miR-7-5p. *BMC Cancer* 2021;21:44.
 29. Chipuk JE, Moldoveanu T, Llambi F, et al. The BCL-2 family reunion. *Mol Cell* 2010;37:299-310.
 30. Ostadrahimi S, Abedi Valugerdi M, Hassan M, et al. miR-1266-5p and miR-185-5p Promote Cell Apoptosis in Human Prostate Cancer Cell Lines. *Asian Pac J Cancer Prev* 2018;19:2305-11.
 31. Bessou M, Lopez J, Gadet R, et al. The apoptosis inhibitor Bcl-xL controls breast cancer cell migration through mitochondria-dependent reactive oxygen species production. *Oncogene* 2020;39:3056-74.
 32. Guo T, Gu C, Li B, et al. Dual inhibition of FGFR4 and BCL-xL inhibits multi-resistant ovarian cancer with BCL2L1 gain. *Aging (Albany NY)* 2021;13:19750-9.
 33. Kyuno D, Takasawa A, Kikuchi S, et al. Role of tight junctions in the epithelial-to-mesenchymal transition of cancer cells. *Biochim Biophys Acta Biomembr* 2021;1863:183503.
 34. Huang Y, Hong W, Wei X. The molecular mechanisms and therapeutic strategies of EMT in tumor progression and metastasis. *J Hematol Oncol* 2022;15:129.

(English Language Editor: A. Kassem)

Cite this article as: Zhang N, Wang F, Zhu L, Chang R, Mok SRS, Peixoto RD, Tang W, Chen Z. Molecular mechanism of the miR-7/BCL2L1/P53 signaling axis regulating the progression of hepatocellular carcinoma. *Ann Transl Med* 2023;11(1):12. doi: 10.21037/atm-22-5929